In Situ Dynamic Measurements of Sol−Gel Processed Thin Chemically Selective PDMDAAC−Silica Films by Spectroscopic Ellipsometry

Imants Zudans, William R. Heineman, and Carl J. Seliskar*

Department of Chemistry, P.O. Box 210172, University of Cincinnati, Cincinnati, Ohio 45221-0172

Received February 25, 2004. Revised Manuscript Received June 3, 2004

Spectroscopic ellipsometry studies of thin sol−gel processed polyelectrolyte−silica composite films used in chemical sensing are presented. Dynamic measurements were used to characterize PDMDAAC−SiO_2 film behavior when equilibrated in 0.1 M KNO_3 solution (supporting electrolyte). Optical modeling of ellipsometric data revealed three transformation phases during the equilibration: (1) a slow initial phase when the film refractive index approached that of the solution while film thickness changed little; (2) the disintegration of the silica xerogel matrix during which the film incorporated a large amount of water expanding to a hydrogel of thickness many times it's original size; (3) the slow dissolution of the swollen hydrogel film. Simultaneous electrochemical studies of the incorporation of $Fe(CN)_6^{3-}$ into films coated on indium tin oxide glass substrates identified the cause of previously observed film failures in sensing applications after long equilibration in aqueous environments.

1. Introduction

Thin chemically selective porous films made by a range of methods are essential parts of many chemical sensors. The composition and function of these films varies depending on the specific sensor type, analytical detection scheme, and designated purpose. Despite the relatively wide use of such films in sensors, literature reports of detailed studies of the physical properties of such thin films are rare. We are developing spectroelectrochemical sensors for detection of a number of environmentally important ions in aqueous media. The concept of the sensor has been described in detail before.[1,2] The base of this sensor is an optical glass substrate that is coated with a transparent, conducting, indium tin oxide (ITO) film that is overcoated with a porous chemically selective film. The function of the chemically selective film is to preconcentrate a target analyte next to the ITO transparent electrode surface. Our sensor currently employs absorbance[1] or fluorescence[3] as a means of quantifying analyte concentration. In such an optical multilayer structure, optimization of the chemically selective film properties is crucial to achieving useful sensor responses to environmentally meaningful analyte concentrations.

To support the applications of interest to us, we developed two broad classes of chemically selective optical quality films. One class is polymer based;[4] the other is sol−gel processed silica-based[5] composites. Both classes of materials rely on forming phase homogeneous composites with ionomers (polyelectrolytes) that impart ion-exchange capacity to the resulting film. Because of a recent successful application of our sensor to a nationally important problem,[6] we have a special interest in the sol−gel processed poly(dimethyldiallylammonium chloride)−silica (herein, PDMDAAC−SiO_2) composite material. Specifically, it was incorporated as a thin chemically selective film in a sensor that was successfully used for detection of ferrocyanide, $Fe(CN)_6^{4-}$, in a very complex, harsh, and radioactive nuclear waste matrix. Unfortunately, the PDMDAAC−SiO_2 composite material undergoes catastrophic breakdown after lengthy equilibration with high-salt and/or high-pH aqueous environments. Despite its obvious shortcomings when used in sensing, this composite material has turned out to be amazingly useful. In an effort to begin to better understand this material, we have begun a detailed investigation of its performance and especially its failures in sensing type environments with the goal of establishing a basis to better design similar but more robust materials.

Spectroscopic ellipsometry has the potential to be used to study, in situ, some of the important dynamic physical properties of thin sensor films. The results of ellipsometric studies are film thickness and optical constants (complex refractive index, $\tilde{n} = n + ik$, as a function of wavelength). While this might at first seem like limited information, such constants give critical insights into changing film dimensions and, through the complex refractive index, changing film composition. In

(1) Shi, Y.; Slaterbeck, A. F.; Seliskar, C. J.; Heineman, W. R. *Anal. Chem.* **1997**, *69*, 3679−3686.
(2) Heineman, W. R.; Seliskar, C. J.; Richardson, J. N. *Aust. J. Chem.* **2003**, *56*, 93−102.
(3) Kaval, N.; Seliskar, C. J.; Heineman, W. R. *Anal. Chem.* **2003**, *75*, 6334−6340.
(4) Gao, L.; Seliskar, C. J. *Chem. Mater.* **1998**, *10*, 2481−2489.
(5) Shi, Y.; Seliskar, C. J. *Chem. Mater.* **1997**, *9*, 821−829.
(6) Stegemiller, M. L.; Heineman, W. R.; Seliskar, C. J.; Ridgway, T. H.; Bryan, S. A.; Hubler, T.; Sell, R. L. *Environ. Sci. Technol.* **2003**, *37*, 123−130.

10.1021/cm049709l CCC: $27.50
Published on Web 07/21/2004

situ ellipsometric studies of thin film swelling have been reported before. Papanu et al. studied[7−9] swelling and dissolution of poly(methyl methacrylate) films in various solvents as well as the rates and mechanisms of these processes. Tang et al. used spectroscopic ellipsometry for characterization[10,11] of various polymer and blended polymer film behaviors. They were able to correlate film composition and annealing affects with the film equilibration process in water. Swelling of polymer brushes (on different surfaces) has been studied by several groups.[12−15] Several groups have used in situ ellipsometry to study film swelling upon exposure to air with varied levels of humidity[16−18] or vapor pressures of solvents.[19,20] We present here a study of the dynamics of sol−gel processed PDMDAAC−SiO_2 composite films during equilibration with and as they ultimately collapse in an aqueous medium. To our knowledge, spectroscopic ellipsometry has not been used for such an application before.

2. Experimental Section

2.1. Chemicals and Materials. The following chemicals were used as received: tetraethyl orthosilicate (TEOS, 99%), poly(dimethyldiallylammonium chloride) polymer (PDMDAAC, molecular weight 200 000−350 000, 20 wt % solution in water) (both from Aldrich), and hydrochloric acid and potassium nitrate (both from Fisher Scientific Co.). Deionized water was prepared with a Barnstead water purification system and used to prepare all solutions.

Liquid cell gaskets were cut from silicone sheeting (0.010 in. thick, gloss/gloss surfaces, Specialty Manufacturing, Inc., Saginaw, MI). Nalgene 50 silicone tubing (0.125 in. i.d. × 0.250 in. o.d., Fisher Scientific) was used to deliver solutions into the ellipsometry cell. Millipore nylon syringe filters (0.45 μm) were used for filtration. Fine annealed Schott SF11 glass substrates (n_d^{20}=1.78, 38 mm × 12 mm × 8 mm, surface quality 40/20, accuracy λ/4, parallelism < 15 arc s) were prepared by MK Photonics, Inc. 1737 F glass (n_d^{20}=1.52, 1 mm thick) and ITO-coated (135 nm thickness) 1737 F glass were purchased from Thin Film Devices and cut into 45 mm × 15 mm pieces. Soda lime glass (n_d^{20}=1.53, 1 in. × 3 in.) microscope slides were used instead of 1737 F glass for initial studies. All SF11 glass substrates, 1737 F glass pieces, and soda lime glass microscope slides will further be referred to simply as *slides*.

2.2. Preparation of Films on Substrates. Films were prepared according to a previously reported procedure.[5,21] Very briefly, a silica sol was prepared by combining in a vial TEOS (4.0 mL), deionized water (2.0 mL), and 0.1 M HCl (100 μL) and stirring this mixture at room temperature for 3 h. PDMDAAC was incorporated into the silica sol by blending a 5% polyelectrolyte solution (4.0 mL) with the sol (3 mL). This final mixture was filtered, ultrasonicated to get rid of air bubbles, and then spin coated (2000 rpm, 30 s) onto SF11 glass substrates, 1737 F glass slides, microscope slides, or ITO−glass slides using a Headway photoresist spinner. Films prepared in such a manner are typically 700−900 nm thick. Slides were dried at room temperature and humidity for at least 1 day before use unless specified otherwise.

2.3. Ellipsometry Procedures. A J. A. Woollam Inc. variable-angle spectroscopic ellipsometer (vertical setup) was used for all ellipsometry measurements. This instrument was equipped with an adjustable retarder (Auto Retarder) that was used in precise mode for non-time-based experiments and in fast mode for dynamic experiments. In both modes measurements of Ψ and Δ were made over the full angular range (0−90° and 0−360°, respectively). However, depolarization of light was not measured in fast mode. Woollam Wvase32 software was used for modeling ellipsometric data using published techniques.[22,23] The liquid cell for ellipsometry was operated under nonflow conditions.

2.4. Electrochemistry Procedures. Electrochemical measurements were performed with a Bioanalytical Systems BAS 100-B electrochemical workstation. A disposable glass vial (28 × 57 mm, 22 mL, Fisher) was used as the electrochemical cell.[24] A cap for this cell was machined with holes for insertion of electrodes. An Ag/AgCl (3 M NaCl) electrode and platinum mesh served as the reference and auxiliary electrodes, respectively. Film-coated ITO−glass slides were soaked for specified lengths of time in 0.1 M KNO_3 solution and transferred to the electrochemical cell (only the reverse side was blotted) containing an aqueous solution of 1 mM potassium ferricyanide and 0.1 M KNO_3. Films were allowed to equilibrate with this solution for 10 min. This time was sufficient for ferricyanide to equilibrate with the film as two consecutive cyclic voltammograms yielded comparable peak currents. After this equilibration period, a voltammogram was recorded with a scan rate of 5 mV/s from 600 to −600 mV. Later in the text we refer to this electrochemistry procedure simply as *tests*.

3. Results and Discussion

Ellipsometry uses plane-polarized light, and in this method Ψ and Δ are the two measured parameters (ellipsometric angles) that quantify the relative phase shift and the intensity change of p- and s-polarized light induced on reflection by the sample. These parameters depend on the detailed optical structure of the sample and, in this case, the layered structure of the sample, the thickness of each layer, and the complex refractive index, $\tilde{n}$, of each layer. Optical modeling enables deconvolution of the optical constants of practical interest from measured Ψ and Δ values. In spectroscopic ellipsometry, the sample is interrogated at many wavelengths. In turn, this enables characterization of more complex samples and also improves the accuracy of data interpretation. For a detailed explanation of data in-

(7) Papanu, J. S.; Soane, D. S.; Bell, A. T.; Hess, D. W. *J. Appl. Polym. Sci.* **1989**, *38*, 859−885.
(8) Papanu, J. S.; Hess, D. W.; Soane, D. S.; Bell, A. T. *J. Appl. Polym. Sci.* **1990**, *39*, 803−823.
(9) Papanu, J. S.; Hess, D. W.; Soane, D. S.; Bell, A. T. *J. Electrochem. Soc.* **1989**, *136*, 3077−3083.
(10) Tang, Y.; Lu, J. R.; Lewis, A. L.; Vick, T. A.; Stratford, P. W. *Macromolecules* **2001**, *34*, 8768−8776.
(11) Tang, Y.; Lu, J. R.; Lewis, A. L.; Vick, T. A.; Stratford, P. W. *Macromolecules* **2002**, *35*, 3955−3964.
(12) Peez, R. F.; Dermody, D. L.; Franchina, J. G.; Jones, S. J.; Bruening, M. L.; Bergbreiter, D. E.; Crooks, R. M. *Langmuir* **1998**, *14*, 4232−4237.
(13) Biesalski, M.; Ruehe, J. *Macromolecules* **2002**, *35*, 499−507.
(14) Currie, E. P. K.; Sieval, A. B.; Fleer, G. J.; Stuart, M. A. C. *Langmuir* **2000**, *16*, 8324−8333.
(15) Biesalski, M.; Johannsmann, D.; Ruhe, J. *J. Chem. Phys.* **2002**, *117*, 4988−4994.
(16) Kugler, R.; Schmitt, J.; Knoll, W. *Macromol. Chem. Phys.* **2002**, *203*, 413−419.
(17) Mathe, G.; Albersdoerfer, A.; Neumaier, K. R.; Sackmann, E. *Langmuir* **1999**, *15*, 8726−8735.
(18) Chen, W.-L.; Shull, K. R.; Papatheodorou, T.; Styrkas, D. A.; Keddie, J. L. *Macromolecules* **1999**, *32*, 136−144.
(19) Sirard, S. M.; Green, P. F.; Johnston, K. P. *J. Phys. Chem. B* **2001**, *105*, 766−772.
(20) Spaeth, K.; Kraus, G.; Gauglitz, G. *Fresenius' J. Anal. Chem.* **1997**, *357*, 292−296.
(21) Gao, L.; Seliskar, C. J.; Heineman, W. R. *Anal. Chem.* **1999**, *71*, 4061−4068.
(22) Woollam, J. A.; Johs, B.; Herzinger, C. M.; Hilfiker, J.; Synowicki, R.; Bungay, C. L. *Crit. Rev. Opt. Sci. Technol.* **1999**, *CR72*, 3−28.
(23) Johs, B.; Woollam, J. A.; Herzinger, C. M.; Hilfiker, J.; Synowicki, R.; Bungay, C. L. *Crit. Rev. Opt. Sci. Technol.* **1999**, *CR72*, 29−58.
(24) Paddock, J. R.; Imants, Z.; Seliskar C. J.; Heineman, W. R. *Appl. Spectrosc.* **2004**, *58*, 608−612.

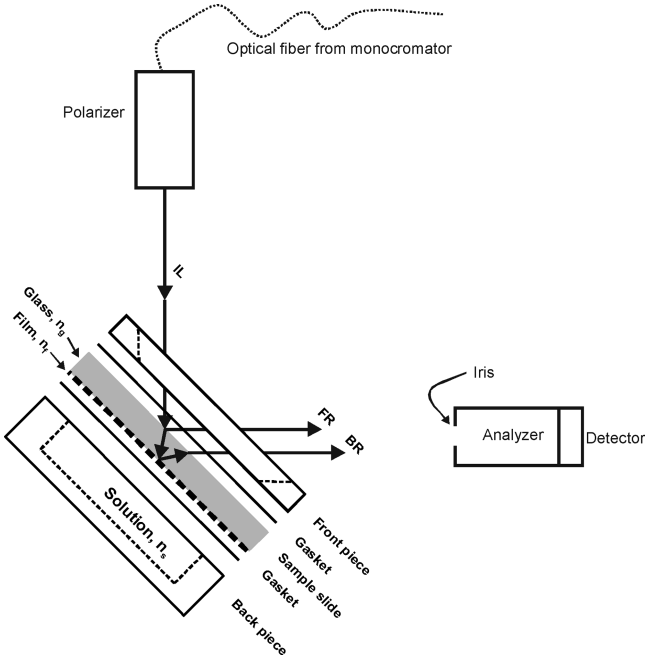

Figure 1. Liquid cell and optical paths for backside ellipsometry. The liquid cell consists of two main parts, and the glass substrate (slide) is placed between them as shown. The back portion of the cell (back piece) has a cavity with two injection ports for liquid flow into and out of the cell. When the cell is assembled as shown, the cavity forms a reservoir for liquid that the film coated on the glass substrate is exposed to. The cell front piece has a cutout in the center to allow light to probe the glass substrate with the film coated on it. Incident light (IL) strikes the front surface of the glass substrate where it is partially reflected (FR) and partially transmitted into the substrate. The transmitted beam then encounters the backside of the substrate where the film resides and is partially reflected back into the glass (and partially escapes as a transmitted beam). This reflected beam travels back to the substrate's front surface where a portion of it escapes as beam BR1 (simply noted as BR). At this interface reflected light continues to multiply reflect in the substrate leading to beams TB2, BR2, etc. (not shown).

terpretation, the reader is referred to literature sources.[22,23,25]

3.1. Dynamic Ellipsometry Measurements. 3.1.1. Liquid Cell. Design and testing of a liquid cell for spectroscopic ellipsometry was described in our publication on ITO film acid etching studies.[26] A smaller version of the liquid cell described there was also made for these studies, and both liquid cells were used in the studies presented here. Later in the text we refer to experiments with a slide mounted in the liquid cell as in situ experiments; all other experiments are termed ex situ.

The principles of the backside interrogation have been presented in detail previously.[27,28] Figure 1 illustrates reflection of the incident light (IL) beam at the sample surfaces with the concomitant formation of reflected and transmitted beams. Reflection that is formed at the front or substrate surface (FR) does not encounter the selective film and, therefore, contains no information about it. Light that has been transmitted into the substrate is eventually partially reflected at the glass/solution interface ultimately emerging from the glass substrate as a series of beams (BR1, BR2, ...). Because the glass substrate side facing solution is coated with the selective film, these beams carry information about film properties. The distance between the front surface reflection (FR) and back reflections (BR1, BR2, ...) is a function of the glass refractive index and the angle of incidence of the light. Depending on the beam diameter and thickness of the glass substrate, it is possible to separate these beams from each other. For example, with a SF11 glass substrate (8 mm thick, high refractive index) complete separation of these beams is achieved and beam BR1 (simply designated BR in Figure 1) can be measured alone, allowing maximum film information to be gleaned from measurements. However, when 1 mm thick glass substrates were used, all beams overlapped and all entered the detector together.

3.1.2 General Optical Model Formulation. Prior to interpretation of dynamically acquired data for films, it is important to characterize the sample as a multilayer optical system. A stepwise approach outlined previously[27,28] was followed. Each different glass substrate was fully characterized before coating with films. For subsequent analyses of film-coated glass slides, the substrate's refractive index was typically used without adjustment. However, for some film-coated slides the ellipsometric data interpretation is very sensitive to the substrate's optical constants. Thus, occasionally very minor variation of the substrate constants was allowed in the computational refinement of the optical multilayer model used. These adjustments are very small in magnitude and should be viewed as fine-tuning of ex-situ-determined values.

Prior to dynamic experiments each film-coated slide was examined ex situ to determine the dry film optical constants and thickness. Slides were also remeasured when they were mounted in the liquid cell prior to injection of liquid to ensure that stress had not been induced by the sample mounting procedure. In building the overall sample optical model, all films were considered to be isotropic optical layers with uniform properties throughout their thickness. The overall optical model consisted of three main layers: glass substrate, chemically selective film, and solution phase. Typically, a few nanometer thick (depending on the particular substrate) surface roughness layer was included on the glass/air interface.[29] The films studied are not exactly the same thickness all across the film, and in the modeling software the film's thickness nonuniformity feature was used to account for this fact. The real part of the film refractive index, n, was modeled using normal Cauchy dispersion, eq 1

$$n(\lambda) = A + B/\lambda^2 + C/\lambda^4 \qquad (1)$$

where A, B and C are scaling coefficients determined by fitting experimental data and λ is the wavelength of the light. Solution phase was modeled as an isotropic

(25) Tompkins, H. G.; McGahan, W. A. *Spectroscopic Ellipsometry and Reflectometry: a User's Guide*; John Wiley: New York, 1998.
(26) Zudans, I.; Seliskar, C. J.; Heineman, W. R. *Thin Solid Films* **2003**, *426*, 238−245.
(27) Zudans, I.; Heineman, W. R.; Seliskar, C. J. *J. Phys. Chem. B*, in press.
(28) Zudans, I. Ph.D. Thesis, University of Cincinnati, Cincinnati, OH, 2003.
(29) Tompkins, H. G.; Smith, S.; Convey, D. *Surf. Interface Anal.* **2000**, *29*, 845−850.

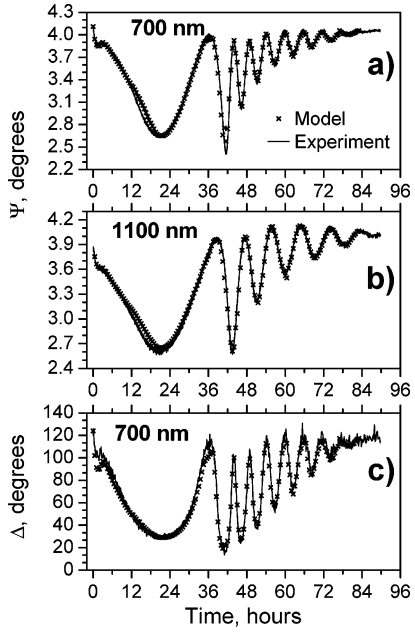

Figure 2. Ellipsometric experimental (solid lines) and optical model (crosses) data (parameters Ψ and Δ) as a function of time at selected wavelengths for a PDMDAAC−SiO_2 film equilibrating in 0.1 M aqueous KNO_3: (a) Ψ at 700 nm; (b) Ψ at 1100 nm; (c) Δ at 700 nm.

layer of maximum software-allowed thickness (10^{20} nm) with a negligibly small value of the constant k ($k = 10^{-9}$) that forced it to behave as a lossless semi-infinite layer in computer refinement calculations.

3.1.3. PDMDAAC−SiO_2 Film Dynamics. Many film samples were studied on several different substrates. High refractive index substrates were always used as previously described[28] to verify the correctness of data interpretation. For any given experiment a huge data set is acquired consisting of individual subsets for each "time slice" of the experiment. For the analysis of the data set presented, the optical model specifically included the following layers: surface roughness (2 nm)−glass (1 mm)−film−solution phase (infinite thickness). The real part of the refractive index of the glass was kept fixed as obtained from ex situ experiments (the extinction was set to zero). Data analysis was performed as follows: one time slice of the data was selected and the software fitting routine was executed, producing film thickness and optical constants that best described that time slice of experimental data. These results were then stored, and the next time slice was analyzed. This sequence was repeated as many times as required to fully resolve the time profile of film properties. Instead of analyzing all the data from the huge data set acquired, it was sufficient in this case to only analyze data acquired at 30 min intervals from the start of the experiment. Determined model parameters with time were then combined, and very limited smoothing was applied using Mathcad 2001 to eliminate spiky data points. Using the parameters from the smoothed data set and the associated optical multilayer model, Ψ and Δ were calculated and compared to experimental results. Figure 2 presents such a comparison at two arbitrarily selected wavelengths (700 and 1100 nm).

Referring to Figure 2 it can be seen that the resultant overall optical model describes the experimental data very well. Some small systematic deviation in Ψ can be

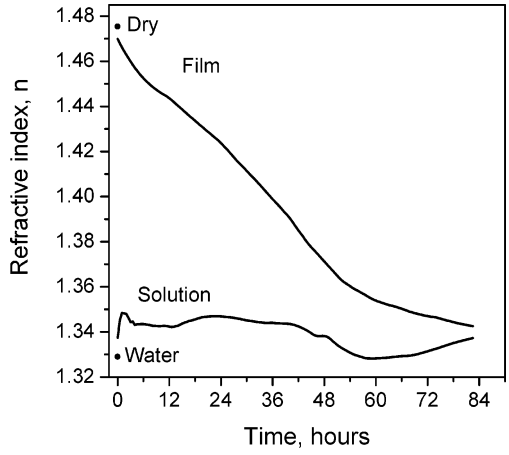

Figure 3. Refractive index, n (700 nm wavelength), of the film and solution layers during the course of film equilibration in 0.1 M aqueous KNO_3. The indices of the dry film and water are included for comparison (shown as dots).

observed between 12 and 18 h. This is a region[28] where the model is least certain and film properties are also somewhat undefined due to its continuing transformation.

Refractive index changes of the solution phase, n_s, and the film, n_f, calculated from fitted parameters at 700 nm wavelength are presented in Figure 3. At other wavelengths these changes are quite similar since the dominant changes in the complex refractive indices reside in the real portions of the indices of these two layers (Cauchy coefficient A) and the changes in the wavelength dispersions of the indices were minimal during the course of the experiment. As the film equilibrated in time, n_f decreased and approached that of the solution. The solution refractive index, n_s, increased slightly in the beginning of the experiment, remaining higher than that of pure water, but decreased toward the end of the equilibration process. We interpret these changes as those of an *apparent* n_s while the real cause of this increase is the formation of a highly swollen layer between the film surface and the solution phase (vide infra). If the optical constants of this swollen layer gradually change from that of the film to that of the solution—and the layer itself is thick and nonuniform—it would be very difficult to detect its presence by ellipsometry. Interestingly, in polymer film swelling studies, the solvent penetration into a film by a moving sharp boundary is called Case II swelling.[7] During such solvent penetration, a swollen layer is formed on the surface of the original film. Formation of a highly swollen surface layer for a PDMDAAC−SiO_2 film is thus similar to Case II swelling; however, solution is also slowly penetrating the bulk film itself ultimately causing film degradation.

From determined thickness values, a *swelling ratio* ρ was calculated as the ratio of film thickness at a particular time (after initial exposure to liquid solution) divided by the dry film thickness (835 nm). Swelling ratio changes during film equilibration are presented in Figure 4. Initially the film thickness slowly decreased slightly, reaching a minimum value after about 20 h. The thickness decrease might be viewed as evidence for the formation of a swollen nonuniform surface roughness layer as the material transitions from dry film to full hydration. If this were the case, then one would

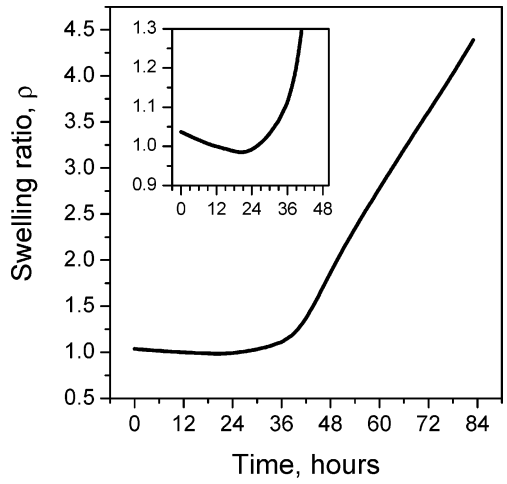

Figure 4. Swelling ratio ρ for a PDMDAAC−SiO_2 film during the course of its equilibration in 0.1 M aqueous KNO_3. (insert) Initial changes in ρ in more detail.

observe such a process as a slight contraction of the main film. This trend was then reversed, and the film started to rapidly increase its thickness as its refractive index continued to approach that of the solution. Such trends are reproducible from film to film. The detailed cause(s) for such remarkable film transformations is not precisely known at present. From a practical standpoint, it is clear that the original film undergoes catastrophic collapse (a breakdown of the initial silica structure that serves as the film backbone or host matrix) and incorporates a large volume of water, which, in turn, leads to a decreased refractive index. It appears that the SiO_2 network which encapsulates the polymer collapses under hydration forces, and the film then forms a new, much thicker hydrogel PDMDAAC film. This highly swollen film can actually be seen by eye when the slide is removed from the liquid cell. Eventually this new hydrogel film completely dissolves if the film remains in solution. It is our current thinking that the driving forces for rapid water uptake and ultimate failure of the silica xerogel host matrix reside in the high hydrophilicity of the ion-exchange polymer PDMDAAC combined with slow dissolution of the host matrix itself.

3.1.4. Visual Data Interpretation. The timed acquisition of spectroscopic ellipsometry measurements leaves one with a huge amount of data that describes film properties in detail. Understanding film transformations requires inspection of these data as a function of both wavelength and time before a suitable optical model can be chosen. One way of handling these large data sets is by plotting experimental data in contour plots. In such plots the ellipsometric angle Ψ or Δ is plotted in wavelength−time coordinates. The value of the angle parameter is then represented by gray-scale intensity. Such data representations are convenient for determination of film transformations and identification of times when critical changes occur. All of this can be done before the laborious task of optical model building and refinement steps.

All Ψ dynamic data for the PDMDAAC−SiO_2 film experiment described above are presented as a Ψ−wavelength−time contour plot in Figure 5a (with inset above). The limited wavelength resolution in this experiment is responsible for the vertical "striations"

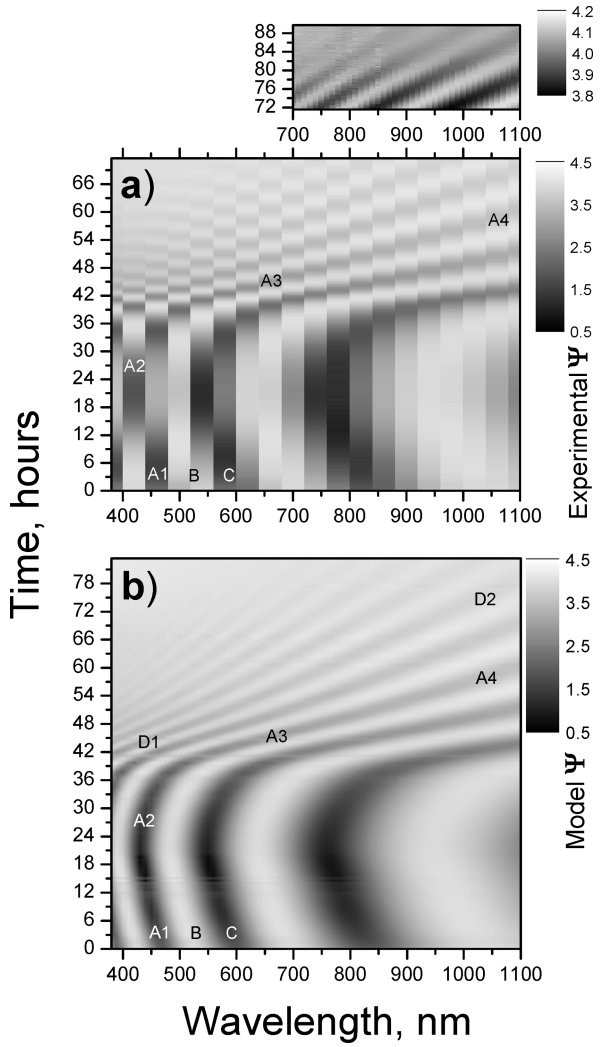

Figure 5. Ψ−wavelength−time contour plot of for a PDMDAAC−SiO_2 film equilibrating in 0.1 M KNO_3: (a) experimental data; (b) data calculated from model fit parameters. Experimental data in panel a shows data from the start of the experiment at 0 to 71.6 h. The wavelength resolution for this potion of the data is 40 nm. After 71.6 h, data acquisition conditions were changed—the wavelength span was narrowed to 700−100 nm and the resolution increased to 10 nm. This portion of the data is presented in the top panel. Ψ values are represented by gray-scale levels as indicated in the scales to the right of the figures. In panel a two minima (darker regions) in Ψ in the beginning of the experiment are marked A1 and C, and a maximum (lighter region) is marked B. As the equilibration progresses, film properties are changing, and these are represented as changes in the Ψ values. The positions of extrema in Ψ shift, and this is represented in the plot as a shift of darker and lighter regions to shorter or longer wavelengths. For example, minimum A first shifts from position A1 to shorter wavelengths—to position A2. As time progresses, this same minimum rapidly shifts to longer wavelengths—to positions A3 and, later, A4.

parallel to the time axis. At later times data (shown as top insert in figure) acquisition conditions were changed by decreasing the scanning wavelength range and increasing the time resolution to better resolve the swollen film changes. Referring to Figure 5a, in the beginning of the equilibration process several minima and maxima in the Ψ−wavelength−time contour can be seen. Two of the minima are labeled in the figure as A1 and C; one maximum is labeled as B. As time progresses these extrema first shift to shorter wave-

lengths (minimum A1 shifts to A2, etc.). These shifts are consistent with both film thickness and refractive index decreases at early times. Minima also became deeper (darker gray), which was especially pronounced for the minimum starting near 850 nm. As equilibration progressed beyond the 30-h mark, extrema shifted to longer wavelengths (minimum A2 shifts to A3 and then to A4, etc.). In addition, new extrema appeared on the short wavelength end of the contour, and this was due to a large film thickness increase. At longer times minima became less shallow (lighter gray, see also top panel insert), and this is consistent with $n_f \rightarrow n_s$. Analysis of the corresponding Δ−wavelength−time contour plot (not shown) proceeds similarly and leads to the same conclusions.

Figure 5b represents a Ψ−wavelength−time contour plot calculated by use of the fully refined optical model for this equilibration experiment. The plot data were calculated with a higher wavelength resolution (10 nm) than the acquired experimental data, and therefore, it is easier to follow the shifts in the extrema. When panels a and b in Figure 5 are superimposed, all features in the contour plots align and it becomes obvious that the overall optical model represents the experimental data very well.

3.2. Concurrent Electrochemistry and Ellipsometry. After studying many PDMDAAC−SiO_2 film equilibrations by ellipsometry, we wanted to correlate film physical changes with the electrochemical behavior that we observed in sensing applications.[6,30,31] Very briefly, while the overall course of equilibration was very similar from film to film, the actual timing of the equilibration stages (hydration, contraction, expansion) was sensitive to many factors. These include, for example, the quality of sol−gel precursor and the film storing conditions (length of drying, ambient humidity). Because some of these factors are hard to control, significant timing variations exist from film preparation batch to batch. Simply put, comparison of films needed to be done within a single batch of prepared samples. In sensing applications we observed that the optimum sensing capacity of PDMDAAC−SiO_2 films was developed about 24−48 h after initial exposure to liquid aqueous media, and this, in turn, meant that the films were somehow time-tuned.[6,30,31]

In an effort to understand this complicated behavior, a study of the electrochemical and physical properties as determined by spectroscopic ellipsometry was launched. In a single batch, many films were prepared on ITO−glass for electrochemical testing and a few were made on glass substrates for ellipsometry. Because all these slides were prepared at the same time from the same PDMDAAC−silica sol blend and dried under identical conditions, it was reasonable to assume that their film transformations in solution would be very similar in timing. One film on glass examined by ellipsometry served as a reference—from ellipsometric data we could determine in which equilibration phase this film was. From these results we, therefore, inferred the status of the remaining films at specific times in their equilibration. PDMDAAC−SiO_2 films adhere very well to both ITO and glass surfaces. Our results suggest that the film itself undergoes large and irreversible changes that ultimately lead to loss of the film from the ITO or glass surface. Because adhesion is sufficiently strong to both surfaces and taking into account that the substrate/film interfacial volume is small compared to the volume of the rest of the film, we conclude that these substrate differences can be neglected.

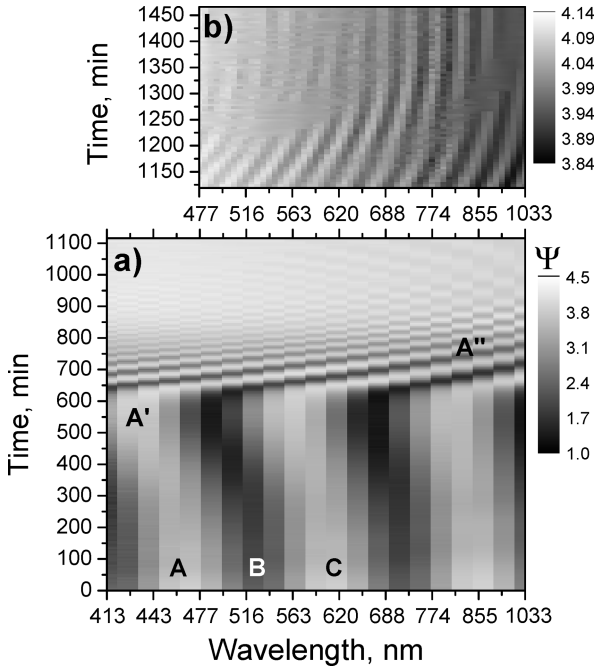

Figure 6. Ψ−wavelength−time contour plot for one PDMDAAC−SiO_2 film (prepared as one of many slides for simultaneous ellipsometry and electrochemistry): (a) initial portion of equilibration in 0.1 M KNO_3; (b) after data acquisition conditions were changed to better resolve film properties. Positions of three extrema in Ψ in the beginning of the equilibration are labeled A, B, and C (see text for discussion).

After an overnight drying, all slides prepared on ITO−glass were placed in a liquid reservoir containing 0.1 M KNO_3 solution (supporting electrolyte solution). One hour prior to this the reference film on glass was exposed to the same solution in the liquid cell and ellipsometry measurements initiated. (Although this sample had dried by 1 h less than the others, this difference is insignificant.) Initially a film on ITO−glass was taken for electrochemical testing every two equilibration hours. At later times in the equilibration, ellipsometry data guided the frequency of these tests. Each test was done with a new sample.

Figure 6 presents the Ψ−wavelength−time contour plots for film equilibration. In the beginning of equilibration there are several easily recognized extrema in the contour—three of them are labeled A−C in panel a. As time progresses, these extrema change positions: point A shifts to A′ and then to A″ and eventually outside the monitored spectral region. Shifts of extrema toward shorter wavelengths are due to film thickness and refractive index decreases. The subsequent rapid shift to longer wavelength is due to film rapid expansion. The number of extrema in the spectral region represented is proportional to film thickness. After time mark 600 min the refractive index of the film approaches that of water, and this is responsible for the

(30) Maizels, M.; Seliskar, C. J.; Heineman, W. R. *Electroanalysis* **2000**, *12*, 1356−1362.
(31) Maizels, M.; Seliskar, C. J.; Heineman, W. R.; Bryan, S. A. *Electroanalysis* **2002**, *14*, 1345−1352.

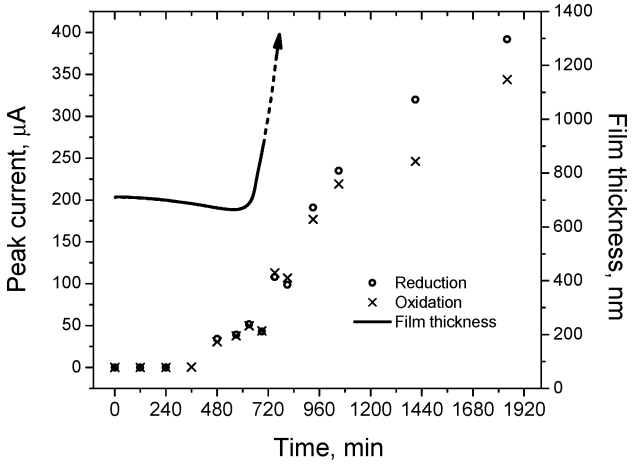

Figure 7. Compound plot of film thickness (solid line) and peak currents (circles and crosses) vs time for a PDMDAAC−SiO_2 film prepared as described in Figure 6.

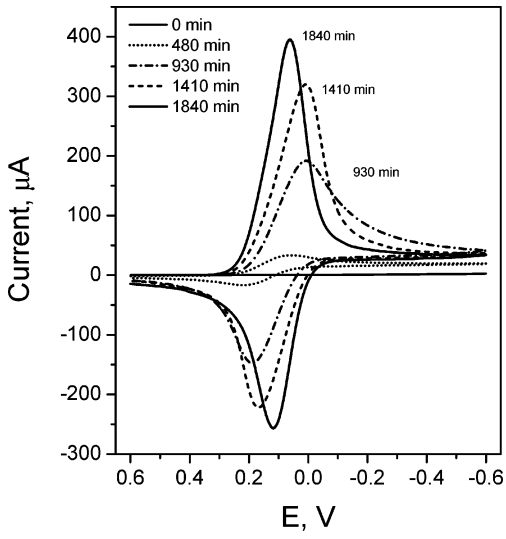

Figure 8. Cyclic voltammograms for a PDMDAAC−SiO_2 film coated on ITO−glass in 1 mM ferricyanide solution recorded at various times of film equilibration in 0.1 M KNO_3 (see legend, Figure 6). Electrochemistry measurements began after 10 min of reequilibration with 1 mM ferricyanide solution. The potential was scanned from +0.6 to −0.6 V vs Ag/AgCl (in 3 M NaCl) at 5 mV/s.

decrease of the difference between minima and maxima in the Ψ−wavelength−time contour. In panel b it can be seen that after about 1300 min of equilibration the extrema stop changing their wavelength positions and approach constant values—a thicker film (as indicated by increased number of extrema compared to the start of equilibration) has been formed that was stable for a fixed period of time.

Film thickness changes for the initial part of the experiment are presented in Figure 7. It can be seen that films made in this batch start to rapidly expand after about 600 min after first contact with solution. At this time extrema in the Ψ−wavelength−time contour have shifted most to short wavelength and, as time progresses, start shifting to longer wavelengths. Data at longer times, shown as the topmost panel of Figure 6 and after experimental ellipsometry conditions were changed to better resolve swollen film changes, reveal another interesting pattern. It can be seen that extrema slowly approach an equilibrium (vertical orientation) and then remain unchanged after about 1300 min. In turn, this suggests that the film has reached a highly swollen (hydrogel) state of relatively stable thickness. This thickness was determined to be ~6.6 times the dry film thickness at the 1200 min mark. However, because fitting of the ellipsometric data is a more complex (and approximate) process for this portion of equilibration data, Figure 7 does not include film thickness changes at these times.

Cyclic voltammograms of films loaded with ferricyanide behaved in a manner that is consistent with the ellipsometry results. Figure 8 shows voltammograms recorded for five films that were each equilibrated for different periods of time ranging from 0 to 1840 min. After equilibration in the supporting electrolyte, they were loaded with ferricyanide by soaking for 10 min in 1 mM ferricyanide in 0.1M KNO_3. Significant changes in the appearance of the voltammograms occur as a result of this soaking.

The shape of a voltammogram for a redox probe loaded into a film on an electrode reflects the relationship between the rate of mass transport of the redox probe in the film to the electrode surface by diffusion (i.e., the diffusion coefficient D_{film}) relative to the thickness of the film in which it is constrained (i.e., the diffusional distance) and the time allowed for diffusion (i.e., the scan rate used to record the voltammogram). When the conditions are dominated by either slow diffusion, short time, or thick film, semi-infinite diffusion prevails. In this case all of the ferricyanide in the film is not electrolyzed during the course of a potential scan. Semi-infinite diffusion voltammograms have a characteristic shape in which the peak potentials are ideally separated by 59 mV (for a 1-electron process) and the current after a peak decays according to $t^{-1/2}$. On the other hand, when conditions are dominated by fast diffusion, long time, or thin film, restricted diffusion prevails. In this case all of the electrochemically accessible ferricyanide in the film undergoes electrolysis during the course of the potential scan. The shape of the restricted diffusion voltammogram is characterized by a peak separation approaching 0 mV and current that shows a sharp drop to a value approaching zero after a peak. In other words, the two peaks are closer together and much sharper.

The voltammograms in Figure 8 show a systematic transition from semi-infinite diffusion behavior to restricted diffusion behavior. No current is recorded for the voltammogram at 0 min because the film is dry and essentially no ferricyande is loaded into the film. Although it is difficult to see because of the current scale used to accommodate all voltammograms in the same figure, the voltammogram at 480 min gives easily measured current and is clearly of the characteristic shape that indicates semi-infinite diffusion on the time scale of the voltammetric scan (480 s). Then as the films are equilibrated for longer times, the voltammograms undergo a transformation in which peak current increases, separation of peak potentials decreases, and peaks sharpen. The increase in peak current can be attributed to either a greater loading of ferricyanide in the film (i.e., increase in C_{film}) or an increase in D_{film} (relative to dry film). However, the decrease in peak separation and sharpening of the peaks is clearly

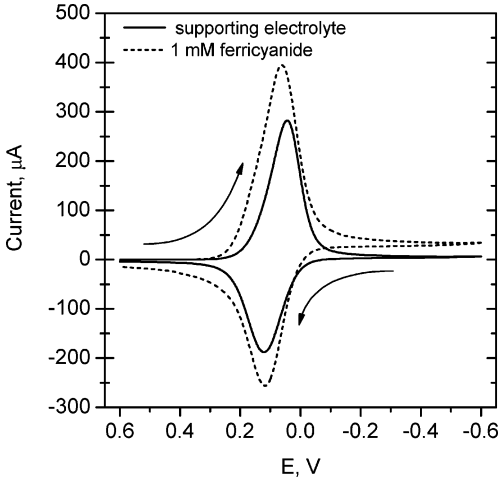

Figure 9. Comparison of two cyclic voltammograms recorded with a film coated on ITO−glass that was equilibrated until its PDMDAAC−SiO_2 film had completely transformed into thicker hydrogel film. The voltammogram in 1 mM $Fe(CN)_6^{3-}$ in 0.1 M KNO_3 solution (dashed line) was recorded during the testing procedure described in the text. Next, that same film-coated slide was removed from $Fe(CN)_6^{3-}$ solution, rinsed with water, and transferred to 0.1 M KNO_3 solution, where the voltammogram shown by a solid line was recorded. Arrows show the direction of the potential scan.

indicative of a transformation from semi-infinite diffusion to restricted diffusion. Given that the time scale is the same for all of the voltammograms, this change can be caused by either an increase in D_{film} or a decrease in film thickness. Because ellipsometry clearly shows that the film is actually increasing in thickness during this time, this phenomenon must be due to a significant increase in the rate of mass transport to the electrode, i.e., an increase in D_{film}. This is consistent with swelling of the film in which the "water channels" increase in size, enabling ferricyanide to move more quickly through the film to the electrode where it undergoes electron transfer. The increase in D_{film} must be sufficiently great to overcome increased film thickness caused by swelling, which works in the opposite way. The correlation between the increase in film thickness measured by ellipsometry and the increase in voltammetric peak currents is clearly shown in Figure 7.

To confirm that recorded voltammograms were primarily due to ferri/ferrocyanide trapped *inside* the film, a film soaked for 1840 min was removed from ferricyanide solution after electrochemistry had been done, gently rinsed with water, and placed in a solution of supporting electrolyte. Figure 9 compares voltammograms recorded at the 1840 min mark in ferricyanide solution (dashed curve) and that obtained after removal and introduction into pure supporting electrolyte solution. Most significantly, the voltammogram recorded in supporting electrolyte exhibits a substantial wave for ferricyanide that was trapped in the film. It is clearly a restricted diffusion voltammogram. The voltammogram recorded in supporting electrolyte has a slightly smaller peak current, indicating that some ferricyanide leached out of the film by the time the voltammogram was recorded. Another difference is that in the reduction wave the peak current returns to zero current for the film in supporting electrolyte while it remains above zero for film in ferricyanide solution. This suggests that

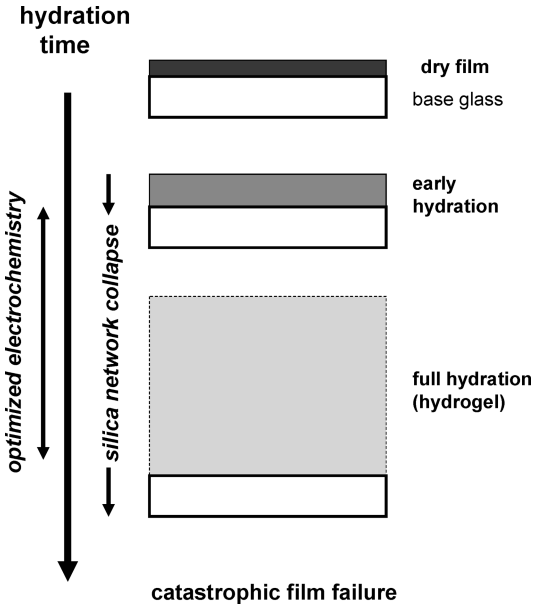

Figure 10. Synopsis of the PDMDAAC−SiO_2 film transformations in time measured by a combination of spectroscopic ellipsometry and electrochemistry.

in addition to ferri/ferrocyanide entrapped in the film, some contribution to the current comes from ferricyanide in adjacent solution that is able to diffuse through the film to the electrode on the time scale of the voltammogram, which is consistent with a more permeable film.

Thus, a clear picture emerges in which the swelling of the film documented by spectroscopic ellipsometry is accompanied by (1) a dramatic increase in D_{film} that accounts for the change in shape of the voltammograms as well as the increase in current and (2) perhaps some increase in C_{film} that contributes to the increase in current but would not influence the characteristic shapes of the voltammograms.

4. Conclusions

The physical and electrochemical changes that ensue when thin PDMDAAC−SiO_2 films anchored on glass (or other oxide surfaces) are exposed to aqueous solution have been measured by a combination of spectroscopic ellipsometry and electrochemistry. Prior to these measurements the failure of such films in sensing applications had been tentatively attributed by us to disappearance of the film from the substrate surface due to poor binding of the film to that surface.[6,30,31] However, the present studies indicate that the main cause for film failure is a transformation within the film itself and not from delamination of the film from the sensor surface.

Hydration of PDMDAAC−SiO_2 films causes remarkable changes within the film itself, and this is illustrated in Figure 10. Introduction of a slight amount of water into the composite leads to a small decrease in film volume. Although we do not currently fully understand why this shrinkage occurs, it might result from initial hydrogen bonding between incorporated water and the polymer, leading to a more compact structure. This slight shrinking of the film is followed by a rapid expansion of the film. This expansion occurs at the expense of the silica host matrix which collapses in

response to the volume change connected to the incorporation of large amounts of water. This incorporation of water is probably driven by the extreme hydrophilicity of PDMDAAC. Concurrent electrochemistry shows that the optimum timing of electrochemical measurements coincides with the rapid expansion and collapse of the silica host matrix. In turn, this suggests that the initially dry PDMDAAC−SiO_2 composite film is a tight network of partially cured silica encapsulating the polymeric phase. The fact that electrochemistry is best done during the hydrogel phase of the film hydration leads us to conclude that the silica matrix acts as an inert phase that is initially too tight for facile diffusion. It also suggests that there may be other matrixes for PDMDAAC better able to withstand the large volume changes of the film on hydration.

Acknowledgment. This work was supported by a grant awarded by the Environmental Management Sciences Program of the U.S. Department of Energy, Office of Environmental Management (Grant DE-FG0799ER62331). The purchase of the J. A. Woollam Inc. spectroscopic ellipsometer was made possible by a grant from the Hayes Fund of the State of Ohio. I.Z. was supported in part by an Ohio Board of Regents Doctoral Investment Award.

CM049709L